

## Author's Accepted Manuscript

The mechanical function of the tibialis posterior muscle and its tendon during locomotion

J.N. Maharaj, A.G. Cresswell, G.A. Lichtwark



PII: S0021-9290(16)30856-9  
DOI: <http://dx.doi.org/10.1016/j.jbiomech.2016.08.006>  
Reference: BM7834

To appear in: *Journal of Biomechanics*

Received date: 2 December 2015  
Revised date: 20 April 2016  
Accepted date: 2 August 2016

Cite this article as: J.N. Maharaj, A.G. Cresswell and G.A. Lichtwark, The mechanical function of the tibialis posterior muscle and its tendon during locomotion, *Journal of Biomechanics*, <http://dx.doi.org/10.1016/j.jbiomech.2016.08.006>

This is a PDF file of an unedited manuscript that has been accepted for publication. As a service to our customers we are providing this early version of the manuscript. The manuscript will undergo copyediting, typesetting, and review of the resulting galley proof before it is published in its final citable form. Please note that during the production process errors may be discovered which could affect the content, and all legal disclaimers that apply to the journal pertain

**Title:** The mechanical function of the tibialis posterior muscle and its tendon during locomotion

**Type:** Original Article.

**Manuscript Number:** BM-D-15-01401

**Revision Number:** 1

**Authors:** J. N. Maharaj, A.G. Cresswell, G.A. Lichtwark

The University of Queensland, School of Human Movement and Nutrition Sciences,  
Centre for Sensorimotor Performance, Brisbane, 4072, Queensland, Australia

**Corresponding author:** Glen Lichtwark

telephone: +61 7 3365 3401

fax: +61 7 3365 6877

email address: g.lichtwark@uq.edu.au

postal address: School of Human Movement and Nutrition Sciences, The University of Queensland, Brisbane, 4072, Queensland, Australia

**Keywords:** walking; elasticity; intramuscular electromyography; muscle; tendon

**Word count:** 3561

The tibialis posterior (TP) muscle is believed to provide mediolateral stability of the subtalar joint during the stance phase of walking as it actively lengthens to resist pronation at foot contact and then actively shortens later in stance to contribute to supination. Because of its anatomical structure of short muscle fibers and long series elastic tissue, we hypothesised that TP would be a strong candidate for energy storage and return. We investigated the potential elastic function of the TP muscle and tendon through simultaneous measurements of muscle fascicle length (ultrasound), muscle tendon unit length (musculoskeletal modeling) and muscle activation (intramuscular electromyography). In early stance, TP fascicles actively shortened as the entire muscle-tendon unit lengthened, resulting in the absorption of energy through stretch of the series elastic tissue. Energy stored in the tendinous tissue from early stance was maintained during mid-stance, although a small amount of energy may have been absorbed via minimal shortening in the series elastic elements and lengthening of TP fascicles. A significant amount of shortening occurred in both the fascicles and muscle-tendon unit in late stance, as the activation of TP decreased and power was generated. The majority of the shortening was attributable to shortening of the tendinous tissue. We conclude that the tendinous tissue of TP serves two primary functions during walking: 1) to buffer the stretch of its fascicles during early stance and 2) to enhance the efficiency of the TP through absorption and return of elastic strain energy.

In human walking and running, elastic energy is known to be stored and returned within the elastic tendinous tissues of muscle-tendon units (MTU) to potentially enhance the efficiency of locomotion (Alexander, 1988; Fukunaga et al., 2001; Lichtwark and Wilson, 2006). In terrestrial animals, the contractile element (i.e. muscle fascicles) of key anti-gravity muscles operate more or less isometrically during early stance (Biewener and Roberts, 2000; Fukunaga et al., 2001; Lichtwark and Wilson, 2006; Roberts et al., 1997). The concurrent stretch of the series elastic element (SEE), which is comprised of tendon, aponeurosis and other connective tissue, contributes the largest component of length increase of the MTU, resulting in absorption of energy within the SEE structures. The absorbed energy is subsequently released to generate the required power during the propulsive phase of late stance, when the MTU shortens rapidly.

Our understanding of the role of elastic tissues during walking has been based primarily on anti-gravity muscles of the lower limbs that act in the sagittal plane and contribute to the forces required for forward progression. However, there is also a requirement to control mediolateral stability (Kuo, 1999), and muscles that cross the hip and the subtalar joint (STJ) are likely to do so (MacKinnon and Winter, 1993). However, to our knowledge, the potential elastic energy contribution of muscles that stabilize frontal plane motion in humans has received little investigation.

The tibialis posterior (TP) MTU is known to contribute to mediolateral stability of the STJ (Otis and Gage, 2001), however its mechanical function during gait is still largely unexplored. Architecturally, the tendinous tissue of the TP is similar to other muscles that are known to store and return elastic energy in their tendons (e.g. human triceps surae). The series elastic tissue runs for most of the MTU length due to the fact that TP consists of relatively short, pennate muscle fibres (fibre length of approximately 2.4 cm and pennation angle of  $11.6^\circ$  in comparison to its MTU length of approximately 25 cm (Wickiewicz et al., 1983). This design appropriately defines it as a 'compliant actuator' (Zajac, 1989). However, the mechanical function of the muscle must also be considered

when assessing whether it might be suitable for storage and return of elastic energy. Intramuscular electromyography (EMG) of the TP during walking suggests that the muscle actively resists STJ pronation during early stance and actively supinates the STJ during late stance (Murley et al., 2009). Kinetic analysis of the STJ reveals a net internal supination moment throughout most of stance (Scott and Winter, 1991). As the TP muscle has the largest supination moment arm about the STJ (Klein et al., 1996) it is likely to actively stretch in early stance and actively shorten in late stance. Given this mechanical function, and the architectural arrangement of the TP muscle, it is possible that the TP muscle utilizes the SEE for the storage and return of energy during walking. However, elastic function of muscles acting in the frontal plane has yet to be explored.

Thus, the aim of this study was to understand the contribution of the TP SEE during walking at different velocities. We hypothesised that TP fascicles would remain relatively isometric while the MTU lengthened and shortened during stance. Direct measurements of TP fascicle length, measured using ultrasound, were combined with motion capture data and modelling to determine muscle-tendon interaction. Intramuscular electromyography of TP was used to determine its pattern of activation.

## **Methods**

Fifteen asymptomatic subjects (9 men, 6 women) with no previous cardiovascular or neurological conditions gave written consent to participate in the study. The subjects' average age, height, and body mass were  $25 \pm 5$  years,  $175 \pm 11$  cm,  $72 \pm 13$  kg, respectively. The protocol was approved by the local university ethics committee and conducted according to the Declaration of Helsinki.

**Experimental protocol.** Participants walked barefoot on a force instrumented, tandem treadmill (DBCEEWI, AMTI, USA) at varying velocities while kinematic, kinetic, muscle activation and ultrasound data were synchronously recorded for the right leg. Walking velocity was normalised to leg length by using Froude number (Fr). Two normalised walking velocities were compared: a)  $Fr = 0.25$  which will be termed the 'preferred'

walking velocity (Minetti et al., 1994); b)  $Fr = 0.4$  which will be termed the 'fast' walking velocity. The mean walking velocity for all subjects was  $1.5 \pm 0.1 \text{ m}\cdot\text{s}^{-1}$  (preferred) and  $1.9 \pm 0.1 \text{ m}\cdot\text{s}^{-1}$  (fast) across the two velocity conditions. The order of walking velocities was randomised and participants were given a 1-min period to accustom themselves to the velocity prior to 15 s of continuous data being collected.

**Motion capture.** Motion data was collected using an eight camera, three-dimensional (3D) opto- electronic motion capture system (Qualysis, Gothenburg, Sweden) at 200 Hz. Infrared reflective markers (14 mm) were placed on specific anatomical landmarks according to a multi-segment foot model developed to describe rear-, mid- and fore-foot motion (Leardini et al., 2007).

**Treadmill data.** Ground reaction forces and moments were collected at 3 kHz from the front and rear force plates mounted beneath the split belts of the treadmill. Participants were required to walk such that each heel-strike landed on the front force plate and toe-off from the rear force plate. This configuration allowed separate left- and right- limb contributions and gait events to be determined.

**Intramuscular electromyography.** Two bipolar fine-wire intramuscular electrodes, each with a 1 mm active recording site, were inserted into TP using a posterior-medial approach at approximately 50% of the distance between the medial malleolus and the medial joint line of the knee (Chapman et al., 2010) under ultrasound guidance (Echoblaster, 128, UAB, Telemed, Vilnius, Lithuania). A single use 0.25 x 40 mm sterilised acupuncture needle (Suzhou Medical Appliance Fact., Suzhou, China) was used as an initial guide. Placement of the electrode was verified by imaging the needle in the muscle before its removal along with the acupuncture needle. The EMG signal was verified using resisted plantar flexion and inversion contractions.

**Ultrasound fascicles images.** TP muscle fascicles were imaged using B-mode ultrasound using the same system described above and a flat-shaped 96-element linear multi-

frequency probe (LV7.5/60/96, Telemed, Vilnius, Lithuania) with a central frequency of 6 MHz, frame rate of 80 Hz and a field of view of 60 x 80 mm (width x depth). Images were collected from the posteriolateral aspect of the leg (Fig. 1).

Musculoskeletal modelling. OpenSim software (Delp et al., 2007) was used to generate a subject specific scaled 3D model. The STJ of a generic 3D musculoskeletal model (Delp, 1990) was modified to a revolute joint with a joint axis of 41° inclination and -23° deviation to the midline of the body, which runs from posterior, inferior and lateral to anterior, superior and medial through the rear-foot (Lewis, 2007). TP MTU length was determined using the geometrical model measuring the distance from the origin on the tibia to the medial aspect of the navicular (defined as a part of the calcaneal segment in the model). The path was constrained using a combination of via points to replicate the function of the flexor retinaculum and a wrapping object (cylinder at the base of the tibia) to model the medial malleolus. The wrapping constraints were chosen to reproduce the flexor-extensor and inversion-eversion moment arms of TP according to Klein (Klein et al., 1996).

Data analysis. Data analysis was performed in Matlab (Mathworks, R2013a, Natick, MA) using custom written scripts. Raw marker positions and ground reaction forces were filtered at the same frequency using a zero-lag second-order low-pass Butterworth filter with a cut-off frequency of 25 Hz which was passed in both the forward and reverse directions. This was necessary to remove noise due to treadmill vibration and to prevent filtering artefact during inverse dynamic analysis (van den Bogert and De Koning, 1996). We used OpenSim's inverse kinematics and inverse dynamic analyses to calculate the STJ angles and moments, respectively.

Fascicle length was defined between the superficial and deep aponeurosis, parallel to the lines of collagenous tissue visible on the ultrasound image and measured using a semi-automated tracking algorithm in MATLAB. This has been shown to be a repeatable and accurate method for estimating fascicle length changes during walking

(Cronin et al., 2011). Ultrasound data from seven subjects were not used for this part of the analysis due to technical problems related to imaging reliable muscle fascicles simultaneously with intramuscular electromyography, leaving complete data sets for 8 participants.

All raw output data (kinematic, kinetic and fascicle) were filtered at a common frequency using a bi-directional, second-order low-pass Butterworth filter with a cut-off frequency of 12 Hz. The STJ angle is reported relative to its angle at heel strike and the average velocity of the STJ was determined by differentiating the average angular displacement with respect to time. STJ power was calculated as the product of the net moment and joint angular velocity at the STJ. The length of the SEE (including tendon and aponeurosis) was determined by subtracting the length of TP fascicles in the direction of the tendon from the change in whole TP MTU length:

$$L_{SEE} = L_{MTU} - L_{Fascicle} \cdot \cos\alpha,$$

where  $L_{SEE}$  is the length of the SEE,  $L_{Fascicle}$  is the length of the muscle fascicle and  $\alpha$  is the pennation angle (Fukunaga et al., 2001, Lichtwark et al., 2007). The length change of the TP MTU, fascicles and SEE were reported relative to their length at heel strike. The mean TP fascicle and MTU velocities were calculated by differentiating the average length with respect to time.

Intramuscular EMG was high pass filtered at 50 Hz. The cut-off frequency was set by visual observation to remove unwanted motion artefact, with the least possible influence on the biological signal. The signal was then rectified, bi-directionally low pass filtered at 6 Hz using a second-order Butterworth filter and normalised to the maximum amplitude recorded at the preferred walking velocity (MAX).

**Statistical Analysis.** Processed kinematic, kinetic, fascicle and EMG data were time-normalised by linear interpolation from right heel strike to ipsilateral heel strike. The stance phase of the gait cycle was subdivided into three periods based on the STJ power curve: negative, zero and positive STJ powers (see Fig. 2C for detail). These

periods were defined when STJ powers either dropped below zero (negative power period) or raised above zero (positive power period). Group means were computed from participant means which were calculated over five strides. Outcome variables (peak TP fascicle and MTU velocities, normalised peak EMG activity and peak STJ power) were calculated for both the negative and positive power periods. Data were tested for normality using a D'Agostino and Pearson omnibus normality tests and differences in each outcome variable between speed conditions were analysed using either a Student's paired t-test, or Wilcoxon's test. The significance level was set as  $P \leq 0.05$ .

## Results

**Subtalar joint mechanics.** During walking at the preferred velocity, the STJ rapidly pronated after heel contact then gradually supinated through mid-stance, while remaining pronated. It then rapidly supinated into supination during late stance (see Figure 2A). The STJ moment increased from heel contact, reaching a maximum during late stance. Mechanical power was absorbed in early stance, remained close to zero during mid-stance before becoming positive during late stance (Fig 2C). The normalised mean  $\pm$  SD peak power absorbed during early stance was  $-0.24 \pm 0.1 \text{ W.kg}^{-1}$ , with returned power in late stance reaching a peak of  $0.24 \pm 0.1 \text{ W.kg}^{-1}$ .

**Muscle mechanics and activity.** At the preferred walking velocity, TP was already active prior to heel contact and reached its first peak of activity ( $46 \pm 7\%$  of MAX) in early stance during the period of negative power, presumably to resist STJ pronation (Fig 3). A second larger peak ( $82 \pm 25\%$  of MAX) occurred in mid-stance, which coincided with the period of positive power and the peak STJ moment (Fig 3). TP activation rapidly reduced during late stance and had low levels of activity through the swing phase.

During stance, TP muscle fascicles differed in their pattern of length change to that of the MTU. During the negative power period, the MTU lengthened by a mean of  $3.6 \pm 1.3 \text{ mm}$ , while its fascicles actively shortened by a mean of  $1.7 \pm 0.3 \text{ mm}$  (see Fig 3). TP

fascicles then slowly lengthened during early mid-stance as the MTU length began to steadily shorten (Fig. 3). During mid-stance, when STJ power was close to zero, minimal length changes of both the MTU and fascicles were evident but coincided to the time when there was a rapid increase in TP activity. During the positive power phase, both the TP MTU and its fascicles shortened as TP activation decreased. Mean peak shortenings during this period were  $3.6 \pm 1.2$  mm in the MTU, and  $4.5 \pm 3.4$  mm in the muscle fascicles.

The lengthening and shortening velocities of the muscle fascicles were also different to those of the MTU during the power absorption and power return periods (Fig. 3). During the power absorption period the MTU lengthened at a mean peak velocity of  $71.2 \pm 23.0$  mm.s<sup>-1</sup> which was significantly faster ( $p \leq 0.01$ ) than the lengthening velocity of the fascicles later during this period at  $24.7 \pm 13.2$  mm.s<sup>-1</sup>. Similarly, during the positive power period the shortening velocity of the MTU reached a maximum of  $-63.3 \pm 31.0$  mm.s<sup>-1</sup> late in this period which was significantly faster ( $p = 0.02$ ) than that of the fascicles, which peaked slightly earlier at  $-29.2 \pm 6.2$  mm.s<sup>-1</sup>.

The estimated length change experienced by the SEE during the stance phase was similar in nature to that of the MTU. In the negative power period the SEE initially lengthened and then began to shorten later in the period. The majority of the SEE shortening occurred during late stance, as both the MTU and fascicles rapidly shortened. As the fascicle shortening velocity was significantly slower than the shortening velocity of the MTU ( $p = 0.02$ ), a substantial component of MTU shortening was due to SEE recoil (Fig. 3).

**Effect of walking velocity.** An increase in walking velocity had a significant effect on muscle and joint mechanics during the power absorption period. At the faster velocity, the STJ absorbed more power ( $p = 0.02$ ) during early stance as indicated by greater negative power. This was associated with a faster peak MTU lengthening velocity ( $p \leq 0.01$ ). The slower shortening velocity of the TP fascicles at the faster velocity was,

however, not significantly different to that at the preferred velocity. The only effect of walking velocity on any measure during the positive power period was a significant increase in TP EMG activity ( $p < 0.01$ ).

## Discussion

Our results clearly demonstrate that during the stance phase of walking, the TP muscle fascicles function more or less isometrically as the SEE recycles power at the STJ. The SEE stretches in early stance, as the muscle fascicles actively shorten, and recoils during late stance to allow the fascicles to shorten at a slower velocity and amplitude than the MTU. This finding is consistent with in-vivo measurements of other anti-gravity muscles that primarily act in the sagittal plane during walking (Fukunaga et al., 2001; Lichtwark and Wilson, 2006). We believe this is the first demonstration of this type of behaviour in muscles that control motion in the frontal plane.

During the stance phase of walking, the SEE of the TP performs negative work to absorb power and positive work to generate power at the STJ. The STJ produces negative power due to a supination moment during STJ pronation, and positive power as it generates supination in the propulsive phase. These periods of power absorption and production are consistent to those calculated using inverse-dynamics in a previous investigation (Scott and Winter, 1991). The STJ performs negative work (time integral of power) during early stance, which is equal in magnitude to the work it produces during propulsion ( $p=0.49$ ). Therefore, the STJ produces minimal net mechanical work over the stance period. We believe this function redirects the centre of mass in both the sagittal and frontal planes during early stance, as explained by the step-to step transition theory by Donelan et al., (2001). The work absorbed at the STJ during early stance by the leading leg may contribute to redirection of the centre of mass in both planes, while the positive work done at the STJ by the trailing leg at push off may replace the energy lost. We believe the elastic function of the TP facilitates this mechanical behaviour.

During early stance, series elasticity acted to absorb energy as the MTU stretched and the muscle generated force, illustrated by the simultaneous increases in the STJ moments and TP EMG activity. At the faster walking velocity, the elastic tissues absorbed more energy; evidenced by the increases in MTU lengthening velocity and EMG activity with minimal change in fascicle shortening velocity. Lengthening of the TP muscle fascicles was evident at the end of the negative power phase, as the MTU and SEE slightly shortened, suggesting that the fascicles absorbed some of the energy stored in the tendon. The SEE therefore buffers stretch in the MTU and decreases the rate of stretch of the fascicles, which may act as a protective mechanism to prevent muscle damage (Konow et al., 2012). In support of this notion, if the fascicles were to absorb all of the stretch of the MTU, it would result in a strain of approximately 16% in each gait cycle and gastrocnemius fascicle strain of 18% during downhill backward walking has been shown to result in moderate post exercise soreness (Hoffman et al., 2013). Therefore, eliminating strains of such magnitude may reduce the potential for TP fascicles to suffer damage.

Although some energy may have been lost during mid stance, where power values were close to zero, a significant amount of energy must have remained stored in the tendon and released during rapid shortening of the MTU in late stance. The majority of SEE shortening occurred as the STJ moment and TP activation diminished. This suggests a drop in TP force, and hence a release of SEE energy, that contributed to positive power productions during push-off. We assume that a large proportion of this positive power is due to recoil of the SEE as the MTU shortened at a much faster velocity than the fascicles. What is unique about our result is that there seems to be a period in the middle of stance where there is very little length change of the MTU and TP fascicles (near zero velocity) while the STJ moment remains high. During this near zero power period we assume that much of the energy stored in the tendon is maintained through sustained activation of TP thereby maintaining force and strain in the tendon. While there is a slight increase in activation prior to the power production phase, this coincided with an increase in the STJ supination moment and may also

reflect slight increases in energy stored in the tendon. While it may seem inefficient to retain energy in the tendon through mid-stance, the alternative, for muscle fascicles to firstly dissipate all energy during early stance and then generate all mechanical work, would be more costly due to increased activation and shortening costs (Lichtwark and Wilson, 2008).

We note that there were some discrepancies between the timing of peak values of the length changes of the SEE and the STJ supination moment. We have assumed that the majority of the supination torque was being generated by TP as it has the largest moment arm at the STJ (Klein et al., 1996). However, other muscles such as the triceps surae and flexor hallucis longus may also contribute to the STJ supination moment (Klein et al., 1996) while co-contraction of the peroneus longus may oppose the STJ supination moment. Therefore, the supination moment may not be indicative of TP force alone. However, given that the stretch of the SEE corresponds with power absorption phase and the shortening corresponds with the power generation phase, we are confident that the TP is the primary contributor to these phases.

There are some further methodological limitations within the current experimental design that need to be acknowledged. During ultrasound recording, it is possible that movement of the probe due to bulging of the triceps surae muscles may cause artefacts to the TP fascicle lengths measured. However, we are confident with our measures based on continuous visibility of fascicles throughout the stride cycle for all subjects. Length changes of the TP MTU are only estimates based on a musculoskeletal model. The OpenSim model used to compute the joint kinematics and consequently the changes in TP MTU length did not have rotating forefoot and midfoot segments, therefore, any length change in MTU that occurred due to rotations about these segments was ignored. The TP also has multiple insertions into the forefoot and midfoot which makes modelling the precise length changes difficult. However, given that relationship between the TP moment arm and STJ angle in our model is similar to that found experimentally in cadaver studies (Klein et al., 1996) we are confident that

the measurements should be within the expected physiological range. We therefore believe that the relative length changes computed from STJ rotations alone were able to adequately illustrate the general behaviour the TP during walking and are accurate estimates to provide an indication of the differences between MTU and fascicle length changes.

### **Conflict of Interest**

The authors declare that they have no conflict of interest, financial or otherwise, related to the materials discussed in this manuscript.

### **Acknowledgements**

J.N. Maharaj is supported by a National Health and Medical Research Council postgraduate scholarship, APP1075000.

### **Conflict of Interest**

The authors declare that they have no conflict of interest, financial or otherwise, related to the materials discussed in this manuscript.

- Alexander, R.M., 1988. *Elastic Mechanisms in Animal Movement*. Cambridge University Press.
- Biewener, A.A., Roberts, T.J., 2000. Muscle and Tendon Contributions to Force, Work, and Elastic Energy Savings: A Comparative Perspective. *Exercise and Sport Sciences Reviews* 28, 99.
- Cronin, N.J., Carty, C.P., Barrett, R.S., Lichtwark, G., 2011. Automatic tracking of medial gastrocnemius fascicle length during human locomotion. *Journal of Applied Physiology* 111, 1491–1496.
- Delp, S.L., Loan, J.P., Hoy, M.G., Zajac, F.E., Topp, E.L., Rosen, J.M., 1990. An interactive graphics-based model of the lower extremity to study orthopaedic surgical procedures. *IEEE Transactions on Biomedical Engineering* 37, 757–767.
- Delp, S.L., Anderson, F.C., Arnold, A.S., Loan, P., Habib, A., John, C.T., Guendelman, E., Thelen, D.G., 2007. OpenSim: open-source software to create and analyze dynamic simulations of movement. *IEEE Transactions on Biomedical Engineering* 54, 1940–1950.
- Donelan, M., Kram, J., Kuo, A. D., 2001. Mechanical and metabolic determinants of the preferred step width in human walking. *Proceedings of the Royal Society of London B Biological Sciences* 268, 1985–1992.
- Fukunaga, T., Kubo, K., Kawakami, Y., Fukashiro, S., Kanehisa, H., Maganaris, C.N., 2001. In vivo behaviour of human muscle tendon during walking. *Proceedings of the Royal Society of London B Biological Sciences* 268, 229–233.
- Hoffman, B.W., Cresswell, A.G., Carroll, T.J., Lichtwark, G.A., 2013. Muscle fascicle strains in human gastrocnemius during backward downhill walking. *Journal of Applied Physiology* 116, 1455–1462
- Klein, P., Mattys, S., Rooze, M., 1996. Moment arm length variations of selected muscles acting on talocrural and subtalar joints during movement: an in vitro study. *Journal of Biomechanics* 29, 21–30.

- Konow, N., Azizi, E., Roberts, T.J., 2012. Muscle power attenuation by tendon during energy dissipation. *Proceedings of the Royal Society of London B Biological Sciences* 279, 1108–1113.
- Kuo, A.D., 2007. The six determinants of gait and the inverted pendulum analogy: A dynamic walking perspective. *Human Movement Science* 26, 617–656.
- Kuo, A.D., 1999. Stabilization of lateral motion in passive dynamic walking. *The International Journal of Robotics Research* 18, 917–930.
- Kuo, A.D., Donelan, J.M., Ruina, A., 2005. Energetic consequences of walking like an inverted pendulum: step-to-step transitions. *Exercise and Sport Sciences Reviews* 33, 88–97.
- Lewis, G. S., Kirby, K.A., Piazza, S. J., 2007. Determination of subtalar joint axis location by restriction of talocrural joint motion. *Gait and Posture* 25, 63–69.
- Lichtwark, G.A., Wilson, A.M., 2008. Optimal muscle fascicle length and tendon stiffness for maximising gastrocnemius efficiency during human walking and running. *Journal of Theoretical Biology* 252, 662–673.
- Lichtwark, G.A., Wilson, A.M., 2006. Interactions between the human gastrocnemius muscle and the Achilles tendon during incline, level and decline locomotion. *Journal of Experimental Biology* 209, 4379–4388.
- MacKinnon, C.D., Winter, D.A., 1993. Control of whole body balance in the frontal plane during human walking. *Journal of Biomechanics* 26, 633–644.
- Murley, G.S., Buldt, A.K., Trump, P.J., Wickham, J.B., 2009. Tibialis posterior EMG activity during barefoot walking in people with neutral foot posture. *Journal of Electromyography and Kinesiology* 19, 69–77.
- Otis, J.C., Gage, T., 2001. Function of the posterior tibial tendon muscle. *Foot and Ankle Clinics of NA* 6, 1–14.
- Roberts, T.J., Marsh, R.L., Weyand, P.G., Taylor, C.R., 1997. Muscular force in running turkeys: the economy of minimizing work. *Science* 275, 1113–1115.
- Scott, S.H., Winter, D.A., 1991. Talocrural and talocalcaneal joint kinematics and kinetics during the stance phase of walking. *Journal of Biomechanics* 24, 743–752.

- van den Bogert, A.J., De Koning, J.J., 1996. On optimal filtering for inverse dynamics analysis, in: Presented at the Proceedings of the IXth Biennial Conference of the Canadian Society for Biomechanics, 214–215.
- Wickiewicz, T.L., Roy, R.R., Powell, P.L., Edgerton, V.R., 1983. Muscle architecture of the human lower limb. *Clinical Orthopaedics and Related Research* 179, 275–283.
- Zajac, F.E., 1989. Muscle and tendon: properties, models, scaling, and application to biomechanics and motor control. *Critical Reviews in Biomedical Engineering* 17, 359–411.

Accepted manuscript

Figure 1: **A.** Image illustrating the anatomy of the tibialis posterior muscle (TP) and the location of the ultrasound transducer and intramuscular electrodes inside it. TP is situated beneath the gastrocnemius (GAS), soleus (SOL) and flexor hallucis longus (FHL) muscles in the posterior compartment of the leg. The intramuscular electrodes were delivered into TP using a posterior medial approach. The ultrasound transducer was orientated along the sagittal plane of the leg, in a similar orientation to the TP fascicles and secured on the leg using a plastic mould and elastic bandage. **B.** Representative ultrasound image of TP. The image illustrates clearly visible TP fascicles located between the deep and superficial aponeurosis (DA and SA, respectively).

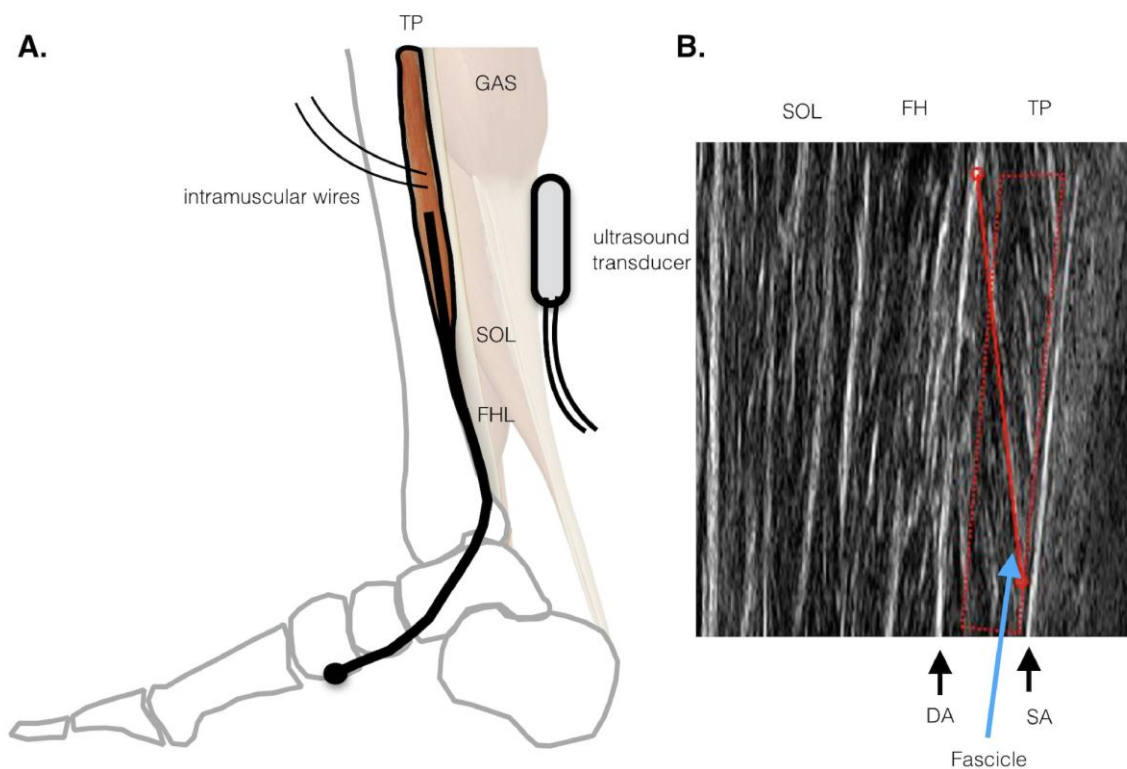


Figure 2: Group mean ( $\pm$  s.e.m.;  $n = 15$ ) time-series data during a stride cycle at the preferred walking velocity for **A.** subtalar joint (STJ) rotation; **B.** normalised STJ moment; **C.** normalised STJ power. Positive values indicate a supinated position, supinatory moments and positive power respectively. The shaded areas indicate negative and positive STJ power phases.

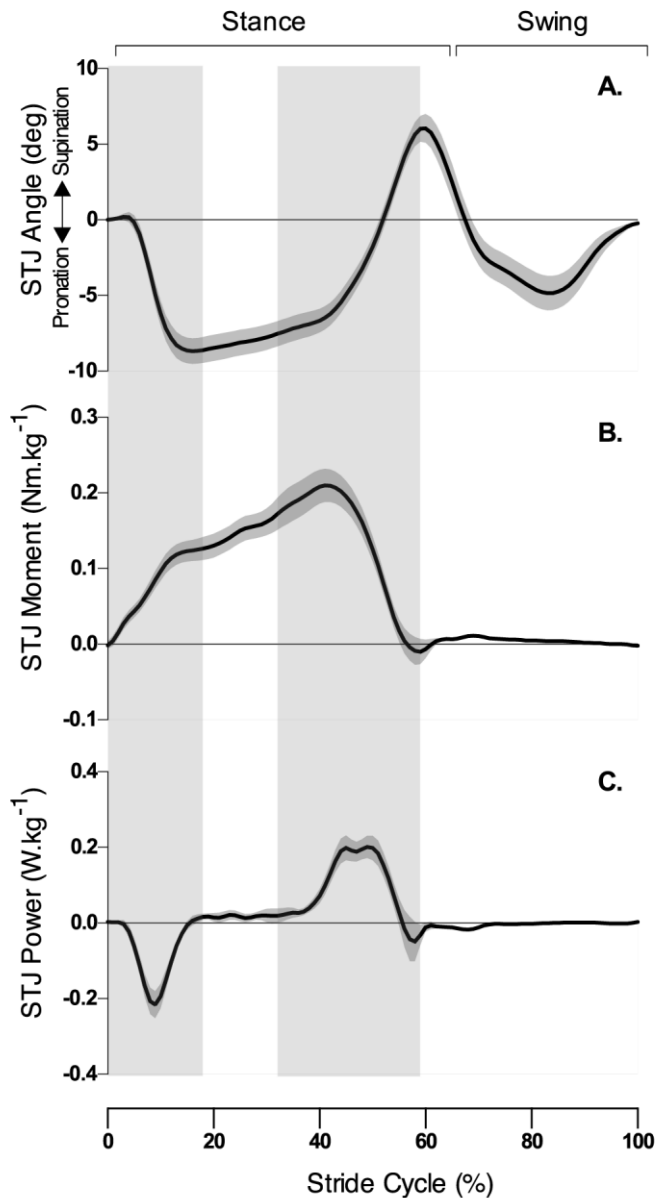
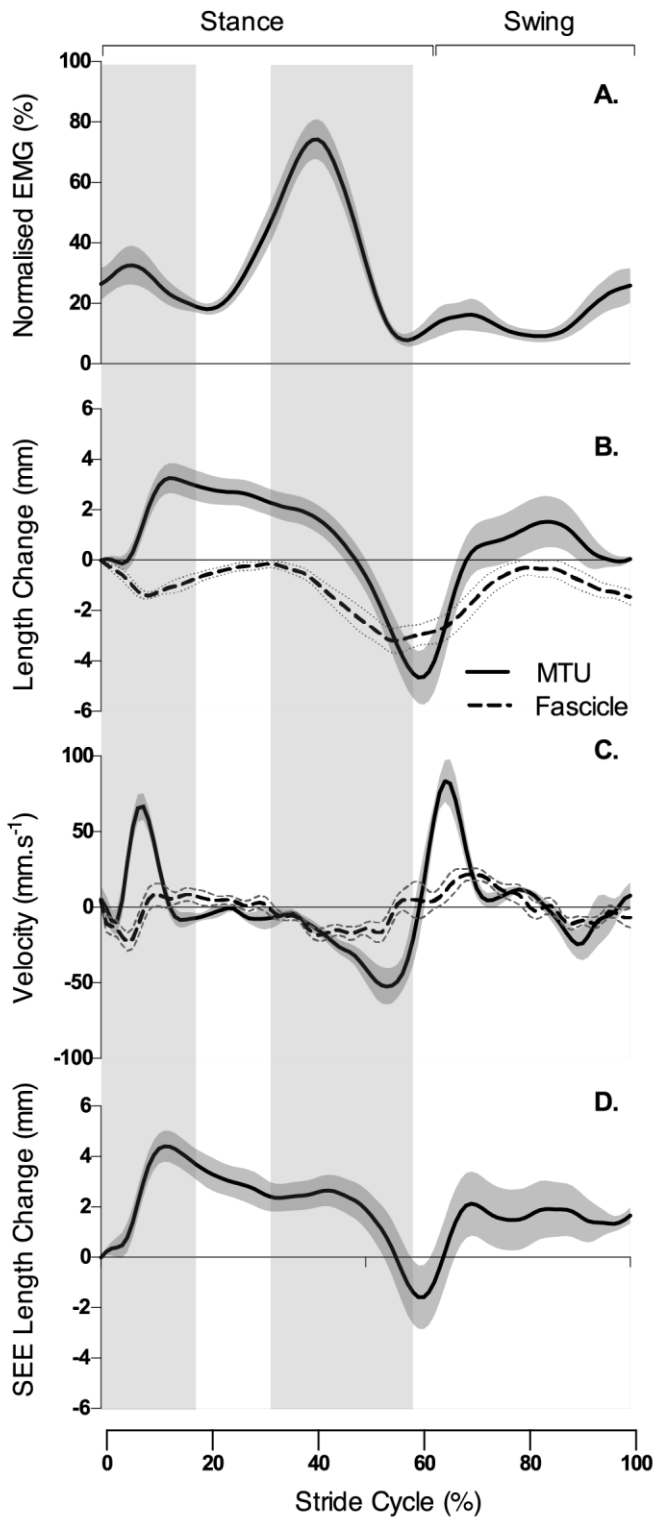


Figure 3: Group mean  $\pm$  s.e.m time-series data during a stride cycle at the preferred walking velocity. **A.** Tibialis posterior (TP) muscle activity normalised to maximum at preferred walking velocity (n = 15); **B.** TP muscle-tendon unit (MTU) length change (solid line) and TP fascicle length change (dashed) relative to heel contact **C.** MTU (solid line) and fascicle (dashed line) velocity; **D.** Series elastic element (SEE) length changes (B, C and D n=8). The shaded areas indicate negative and positive STJ power phases.

Accepted manuscript



Manuscript

Figure 4: Group mean data  $\pm$  s.e.m during negative (filled square, solid line) and positive (open square, dashed line) power phases at the subtalar joint (STJ). **A.** Mean muscle-tendon unit (MTU) velocity **B.** Mean fascicle velocity; **C.** Mean STJ power; and **D.** Peak normalised tibialis posterior (TP) electromyography (EMG). (A, B n=8; C, D n=15). Asterisks (\*) represents statistical significance.

